Title
The observed and simulated major summer climate features in northwest China and their sensitivity to land surface processes

Journal
Journal of Meteorological Research, 28(5)

ISSN
2095-6037

Authors
Li, Qian
Xue, Yongkang

Publication Date
2014-10-01

DOI
10.1007/s13351-014-4010-x

Peer reviewed

The Observed and Simulated Major Summer Climate Features in Northwest China and Their Sensitivity to Land Surface Processes

LI Qian[1*](李 倩) and XUE Yongkang[2,3] (薛永康)

1 *Center for Monsoon System Research, Institute of Atmospheric Physics, Chinese Academy of Sciences, Beijing* 100190, *China*

2 *Department of Geography, University of California, Los Angeles, CA* 90095-1524, *USA*

3 *Department of Atmospheric and Oceanic Sciences, University of California, Los Angeles, CA* 90095-1524, *USA*

(Received January 24, 2014; in final form May 26, 2014)

ABSTRACT

Northwest China (NWC) is a typical arid and semi-arid region. In this study, the main summer climate features over NWC are presented and the performance of an atmospheric general circulation model (NCEP GCM/SSiB) over this region is evaluated. Satellite-derived vegetation products are applied in the model. Based on comparison with observational data and Reanalysis II data, the model generally captures major features of the NWC summer energy balance and circulation. These features include: a high surface temperature center dominating the planetary boundary layer; widespread descending motion; an anticyclone (cyclone) located in the lower and middle (upper) troposphere, covering most parts of central NWC; and the precipitation located mainly in the high elevation areas surrounding NWC.

The sensitivity of the summer energy balance and circulation over NWC and surrounding regions to land surface processes is assessed with specified land cover change. In the sensitivity experiment, the degradation over most parts of NWC, except the Taklimakan desert, decreases the surface-absorbed radiation and leads to weaker surface thermal effects. In northern Xinjiang and surrounding regions, less latent heating causes stronger anomalous lower-level anticyclonic circulation and upper-level cyclonic circulation, leading to less summer precipitation and higher surface temperature. Meanwhile, the dry conditions in the Hexi Corridor produce less change in the latent heat flux. The circulation change to the north of this area plays a dominant role in indirectly changing lower-level cyclonic conditions, producing more convergence, weaker vertical descending motion, and thus an increase in the precipitation over this region.

Key words: Northwest China (NWC), arid and semi-arid regions, atmospheric general circulation model, land cover change, land surface processes

Citation: Li Qian and Xue Yongkang, 2014: The observed and simulated major summer climate features in Northwest China and their sensitivity to land surface processes. *J. Meteor. Res.*, **28**(5), 836–848, doi: 10.1007/s13351-014-4010-x.

1. Introduction

Approximately 50% of the land surface in China is arid or semi-arid, over 80% of which is in Northwest China (NWC) (Dong et al., 2006). NWC is located north of 35°N and west of 107°E, and includes western Inner Mongolia, Gansu Province, Ningxia Hui Autonomous Region, and Xinjiang Uygur Autonomous Region. Most of the land surface in NWC is typically Gobi and desert land with sparse vegetation. In the northern and western mountain areas, the dominant vegetation types are needle-leaf evergreen forest and grassland. The annual precipitation over NWC is less than 50 mm, but annual potential evaporation reaches greater than 3000 mm. As the situation in many arid and semi-arid regions, there is large sensible heat flux in NWC, which is transferred to the atmosphere, affecting the general circulation and the East Asian

Supported by the National Natural Science Foundation of China (41275003 and 41030106), National Basic Research and Development (973) Program of China (2014CB953903), and U.S. National Science Foundation (NSF-ATM-0353606).

*Corresponding author: qian@mail.iap.ac.cn.

monsoon (Bueh et al., 2002; Huang et al., 2006; Zhou and Huang, 2006). Such a region is often called the "thermal pad" in the Eurasian continent (Huang et al., 2006). Despite the above known facts, there have been few studies on the climate variability and sensitivity of NWC to land surface processes. Understanding the climate and environmental change of NWC, as well as the associated physical processes, is a major objective in climate change research in this part of the world.

Despite their usefulness, general circulation models (GCMs) or regional climate models (RCMs) have been only moderately used to study the role of land surface process in the climate change of arid areas in NWC (e.g., Long et al., 2003). One study, which employed the land surface model (LSM) of the National Center for Atmospheric Research (NCAR) (Wang et al., 2002), showed that sensible heat flux is an important part of the energy balance in the arid areas of NWC, but latent heat flux should not be ignored when precipitation occurs. Using a two-dimensional mesoscale soil-plant-atmosphere model, Zhang and Zhao (1998) studied the diurnal variation of soil water and physical variables of leaf surfaces, as well as the spatial surface energy budget distribution over two contrasting surfaces (oasis and desert) in NWC. However, in the above-mentioned model-based studies, land surface processes are not well represented in the models. Long et al. (2003) pointed out that: (1) many land surface parameters used in the models are derived from experiments carried out in humid regions, which produce improper energy and water transfer over arid and semi-arid soils; and (2) rather crude land surface conditions are prescribed in many models for climate studies in NWC (because quite limited observational data are available for descriptions of land surface vegetation characteristics and land surface processes), e.g., the surface bulk transfer coefficient, the ordinary variables on finer spatial and temporal scales, etc. Although a few field experiments have been conducted and some important results are obtained, e.g., the Heihe River basin Field Experiment (HEIFE; Hu and Gao, 1994), they are insufficient for large-scale climate and environmental change studies in NWC.

In this study, we introduce satellite-derived land surface conditions for NWC. Previous studies have indicated the importance of vegetation characteristics, such as leaf area index (LAI), on regional and global climate, and that unrealistic vegetation presentation in GCMs can increase the model bias in the simulation of water and energy transfer between the near-surface atmosphere and land (e.g., Buermann et al., 2001; Friend and Kiang, 2005). Nowadays, more data on these crucial characteristics are available for climate research with the development of remote sensing and retrieval methodologies (Kang et al., 2007). We apply satellite-derived LAI (referred to as RSLAI) in this study on NWC regional climate. Buermann et al. (2001) pointed out that the introduction of RSLAI in the NCAR GCM can improve simulations of near-surface temperature and rainfall over some regions. Meanwhile, experiments by Kang et al. (2007) showed that simulations of near-surface climate in the East Asian summer monsoon regions can be greatly improved by using RSLAI and other satellite-derived land surface data in the NCEP GCM. The present study assesses for the first time the capability of the NCEP GCM by using RSLAI and a satellite-derived vegetation map (Xue et al., 2004) in simulating the climate of NWC.

Another aim of the current work is to evaluate the possible effects of land surface processes on the climatic features of NWC in summer. As the social economy and population density continue to increase in the region, there is evidence that land use and the quality of the environment in NWC are changing considerably, and the surface ecosystem is becoming increasingly fragile (e.g., Xu et al., 2002). The surface vegetation cover has seriously deteriorated in vast parts of NWC since 1995, as identified by multiple sources, e.g., the NOAA's Advanced Very High Resolution Radiometer (AVHRR) and the Television Infrared Observation Satellite's Operational Vertical Sounder (TIROS-TOVS), and as documented in Xu et al. (2007). When land cover changes, land variables such as albedo, surface roughness, and bulk transfer coefficient also change, which leads to variations in surface heat fluxes and ultimately results in surface temperature anomalies. Accordingly, a sensitivity experiment in which the vegetated parts of NWC are altered to bare ground is conducted in the present study. Using dramatic changes to land conditions to evaluate the impacts of land surface processes has been widely used in regional studies. This may also serve as a preliminary platform upon which more comprehensive studies can be built. For example, this method has been applied in land cover change studies over the Amazon (e.g., Shukla et al., 1990), the Sahel (e.g., Xue and Shukla, 1993), and East Asia (e.g., Yatagai and Yasunari, 1995; Xue, 1996; Fu, 2003).

Many statistical analyses and numerical experiments over different regions of China have shown that land cover change exerted great impacts on local precipitation and temperature (e.g., Xue, 1996; Zheng et al., 2002a, b; Ding et al., 2005). For NWC, a correlation analysis with observational data, including reanalysis data from the ECMWF, and NOAA-AVHRR and TIROS-TOVS satellite remote sensing data, showed that the changes in land cover could have resulted in a decrease in total cloud cover and an increase in air temperature, as well as impacts on other regions' climate (Xu et al., 2007). Using the Fifth-Generation Penn State/NCAR Mesoscale Model (MM5), and based on observed data, Chen et al. (2009) examined how the variation in regional climate between the 1970s and 1990s in NWC relates to land cover changes, with a particular focus on the impact on surface temperature and circulation. Although there has been progress in studying the impact of land cover change on the precipitation over NWC, compared with land cover change studies in other regions such as the Sahel, the interacting processes and associated physical processes including the surface energy balance and water balance, are not fully understood for NWC. Therefore, in this study, the effects of land surface processes on the major summer climate features in NWC are preliminarily identified and evaluated by using a land degradation scenario.

The remainder of the paper is structured as follows. The model and experimental design are described in Section 2. In Section 3, we present and discuss the simulated results, in which the capability of the model in using satellite-derived vegetation products to simulate the summer surface energy balance and circulations is highlighted. In Section 4, we discuss how the summer climate features over the NWC are affected by land cover change. Finally, in Section 5, we provide some concluding remarks.

2. Model description and experimental design

In this study, the coupled NCEP GCM/SSiB (Simplified Simple Biosphere; Xue et al., 1991) model is used, which has 28 vertical levels and a T62 (approximately 2°) horizontal resolution. As a forecasting model, the NCEP GCM is also used for climate studies. The fluxes of momentum and surface energy, skin temperature, as well as albedo, are provided to the GCM by the biophysical model, SSiB.

Satellite-derived vegetation products provide several vegetation properties used in the NCEP GCM/SSiB. The satellite product is the Fourier-Adjusted, Sensor and solar zenith angle corrected, Interpolated, Reconstructed Normalized Difference Vegetation Index (FASIR-NDVI), which covers 17 yr from 1982 to 1998 (Los et al., 2000). This dataset includes LAI, vegetation cover infraction (VCI), leaf fraction, and surface roughness length, and is described in detail by Los et al. (2000). Meanwhile, a vegetation map based on satellite observations is used in the NCEP GCM to specify the land cover condition (Hansen et al., 2000; Xue et al., 2004). We refer to this as the SSiB classification map, with a resolution of 1 km^2. When aggregating the vegetation map to the GCM grid points, the cover types are grouped into 12 SSiB vegetation types (Xue et al., 2001), and then the main type is selected in each T62 cell (Fig. 1a).

Using the NCEP GCM/SSiB, we conduct experiments with three different initial conditions, integrated for five months from May to September. The three different initial atmospheric conditions are obtained from the NCEP/NCAR global reanalysis dataset. The ensemble simulated results are then averaged to obtain the final results. The FASIR RSLAI data interpolated from a resolution of 1° to the model grids are used. In this study, the simulated results in the summer season (June, July, and August; JJA) of the ensemble

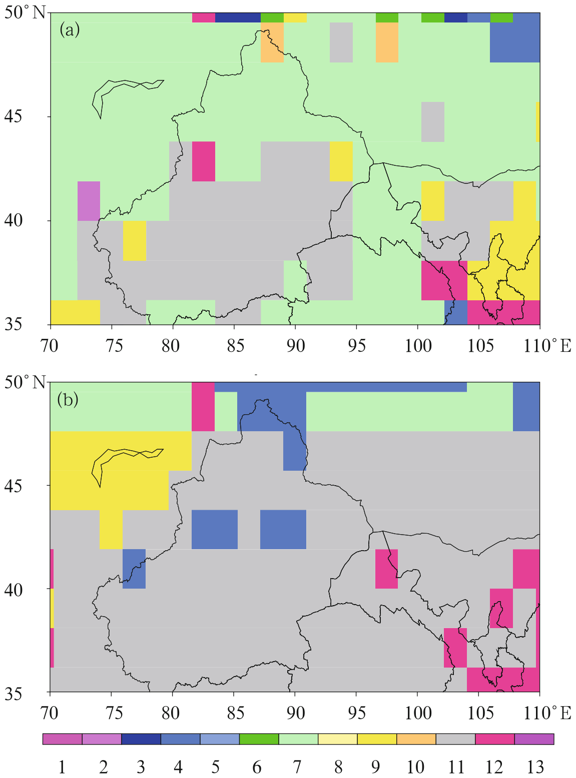

Fig. 1. NCEP GCM/SSiB land cover classification map in Northwest China. (a) SSiB classification map and (b) Kuchler classification map. Type 1: tropical rain forest; type 2: broadleaf deciduous trees; type 3: broadleaf and needle leaf trees; type 4: needle leaf evergreen trees; type 5: needle leaf deciduous trees; type 6: broad leaf trees with ground cover; type 7: grassland; type 8: broadleaf shrubs with ground cover; type 9: broad leaf shrubs with bare soil; type 10: dwarf trees with ground cover; type 11: desert; type 12: crops; type 13: permanent ice.

experiments are averaged. This set of experiments, which uses the SSiB classification map, is referred to as Control, and is evaluated by using the Second Global Soil Wetness Project (GSWP-2; Dirmeyer et al., 2006) data, NCEP/DOE (Department of Energy) Reanalysis II data (Kanamitsu et al., 2002), and also weather station data provided by the National Meteorological Information Center of China (NMICC).

In order to examine the responses of NWC summer climate to land degradation, we conduct an idealized experiment in which the land degradation conditions in the NCEP GCM/SSiB are provided by another vegetation map. We refer to the experiment using the SSiB classification map as case S1 (as in Control, mentioned above), and the experiment based on the land classification of Kuchler (1983) and Matthews (1984, 1985) as case S2 (referred to as the Kuchler classification map; Fig. 1b).

Over NWC and the surrounding areas, significant differences exist between the two classification maps (SSiB and Kuchler). In the SSiB classification, the land cover type is assigned as grassland and shrubland as well as desert in central-southern Xinjiang, which is close to reality (Chen, 1994). However, the whole of NWC is classified as desert in the Kuchler classification. In the land degradation experiment, vegetation parameters such as LAI over the land degradation areas are changed and assigned from a table based on vegetation types (Dormen and Sellers, 1989; Xue et al., 1996). We use the two different classification maps to obtain the maximum response of land cover change. The results from this preliminary experiment should provide useful information regarding the impact and mechanisms involved, constituting a helpful step for more realistic assessments in the future. In addition, since the Kuchler classification has been used in previous GCM studies (e.g., Xue et al., 1991), the difference between these two cases also indicates simulation uncertainty due to improper specification of land conditions. The only difference between the S1 and S2 experiments is the different vegetation maps used.

3. General features of NWC summer climate and their simulation

The major summer circulation and other climate features of NWC have been reported by a number of diagnostic studies (e.g., Wu and Qian, 1996). Sensible heat release and strong downward flow from the northern slope of the Tibetan Plateau (TP) make NWC a significant summer "thermal pad," when the planetary boundary layer is dominated by a high surface temperature center and widespread descending motion in the troposphere over the region. In this section, the major characteristics of the surface energy balance, surface temperature, vertical motion, vorticity fields, precipitation over NWC, and their simulation, are presented and discussed.

3.1 Evaluation of the NCEP GCM/SSiB

The land skin temperature in NWC, especially the Taklimakan desert, Badain Jaran desert, Tengger desert, and the surrounding Gobi area, is extremely high during daytime in spring and summer due to little cloud cover, abnormally low humidity ($< 20\%$), and high solar radiation (Zhou and Huang, 2008). According to the GSWP-2, NMICC, and Reanalysis II data, a high skin temperature center is located in NWC in summer. Meanwhile, the temperature along the southern boundary of NWC has a sharp gradient due to the cold temperature of the TP (Figs. 2a–c). The NCEP GCM/SSiB produced this skin temperature feature, including the warmest centers located in the Taklimakan and Badain Jaran deserts (Fig. 2d). The temperatures simulated by the NCEP GCM/SSiB are much closer to the NMICC data (Fig. 2b), which are higher than the Reanalysis II data by 8–10℃. The 2-m air temperature has the same pattern over NWC (figure omitted), consistent with the surface skin temperature field.

3.2 Surface energy balance

The high albedo of deserts and Gobi reflects a large amount of solar radiation over NWC. Furthermore, the high skin temperature also leads to large amounts of surface upward longwave radiation (figure omitted), which produces a low surface net radiation center in summer over NWC (Figs. 3a and 3b). Since the surface energy balance variables in Reanalysis II data are not so reliable, here we only use the GSWP-2 data for evaluation. The NCEP GCM/SSiB simulates only one low center over the whole region (Fig. 3a). Meanwhile, large sensible heat flux is released to the atmosphere, which accounts for approximately 75% of net radiation (Figs. 3c and 3d). Although intensity differences in the net radiation and sensible heat flux have been reported in some studies based on reanalysis

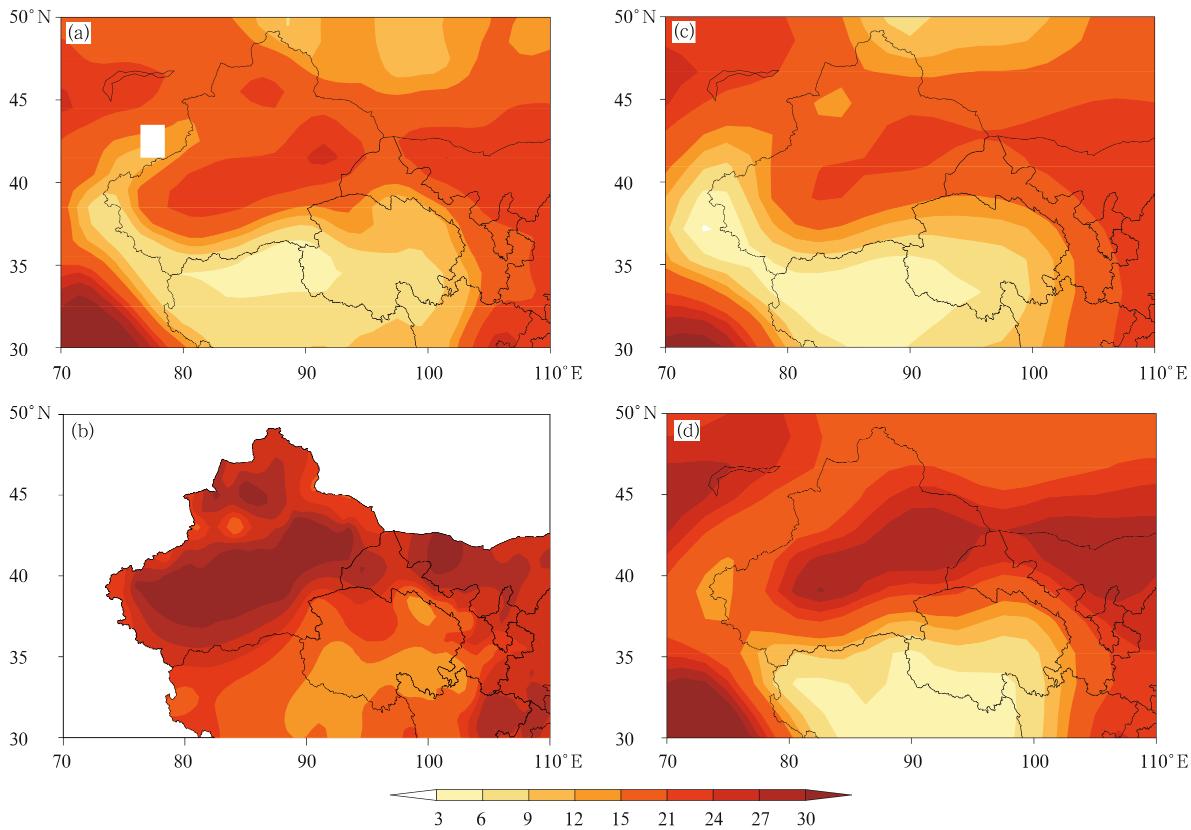

Fig. 2. JJA mean surface temperature (℃). (a) GSWP-2, (b) Reanalysis II, (c) NMICC observational data, and (d) NCEP GCM/SSiB.

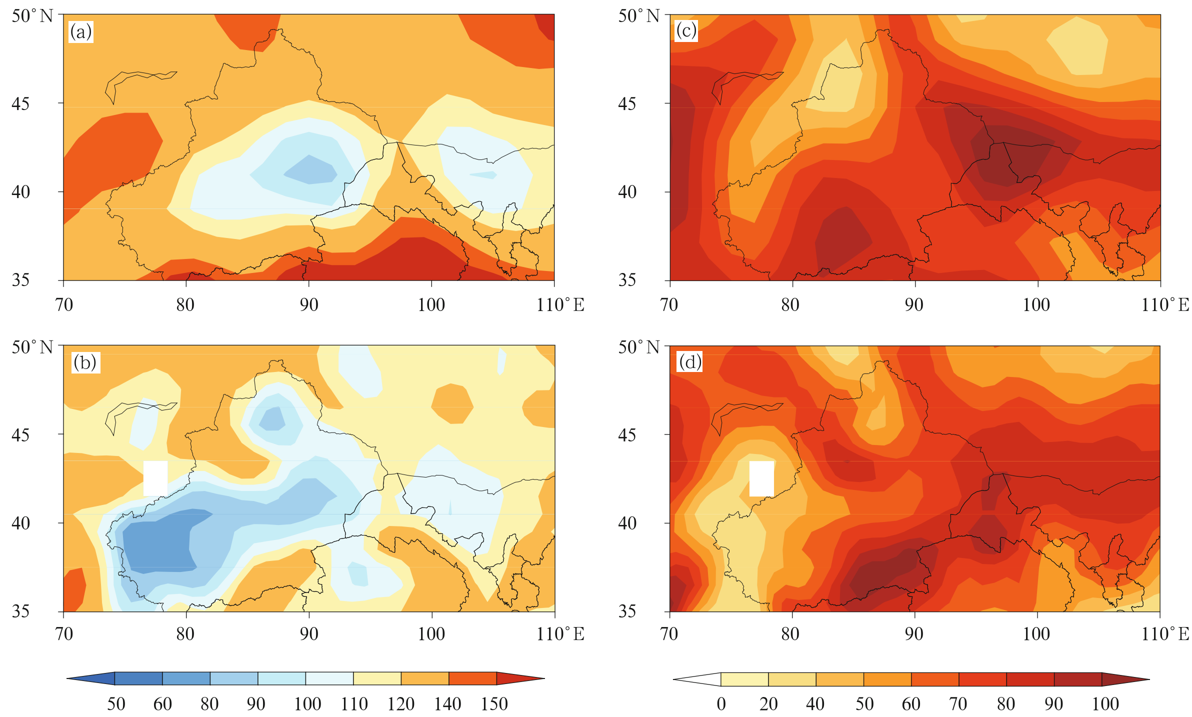

Fig. 3. JJA mean (a, b) surface net radiation (W m^{-2}) and (c, d) sensible heat flux (W m^{-2}). (a, c) NCEP GCM/SSiB and (b, d) GSWP-2.

and observational data (e.g., Zhou, 2009), the stronger effect of the "thermal pad" over NWC is still illustrated by the NCEP GCM/SSiB results.

3.3 Vertical motion and vorticity fields

Over the southern part of NWC, ascending vertical motion occurs in the entire troposphere, which is related to vertical airflow over the TP. Meanwhile, accompanying subsiding currents occur to the north of the plateau (Fig. 4a), covering central and northern Xinjiang Uygur Autonomous Region, northwestern Gansu Province, and Inner Mongolian Autonomous Region, as well as some parts of other central Asian countries.

The NCEP GCM/SSiB simulates the widespread descending and ascending motion at 500 hPa over the above-mentioned areas. However, there are two descending centers over NWC at 500 hPa in the Reanalysis II data (Fig. 4a): one over the north of Xinjiang Uygur Autonomous Region, and the other over Inner Mongolian Autonomous Region. The model results, however, only show one descending motion center (Fig. 4b), and with much stronger intensity. The vertical motion at 700 hPa has the same pattern as at 500 hPa (figure omitted).

There are strong anticyclonic circulations associated with the descending motion in the lower layer, as well as a strong and stable cyclonic convergence center at upper levels. The Reanalysis II divergence field at 200 hPa shows a wide cyclonic band with its center located in the northern part of NWC (Fig. 5a). The NCEP GCM/SSiB simulates the strong cyclone; however, it moves to the northwest (Fig. 5b). At 500 hPa, the Reanalysis II data show a wide anticyclone band from Xinjiang to Inner Mongolia, with its center located over the Taklimakan desert (Fig. 5d). The NCEP GCM/SSiB produces this pattern, but with stronger intensity (Fig. 5e). The NCEP GCM/SSiB model also captures the key circulation feature on the northern side of the TP; in particular, the Asian jet structure in summer, which can clearly be seen in Fig. 5.

3.4 Precipitation

Figure 6a shows the JJA observed rainfall data based on 6-yr daily weather station data provided by

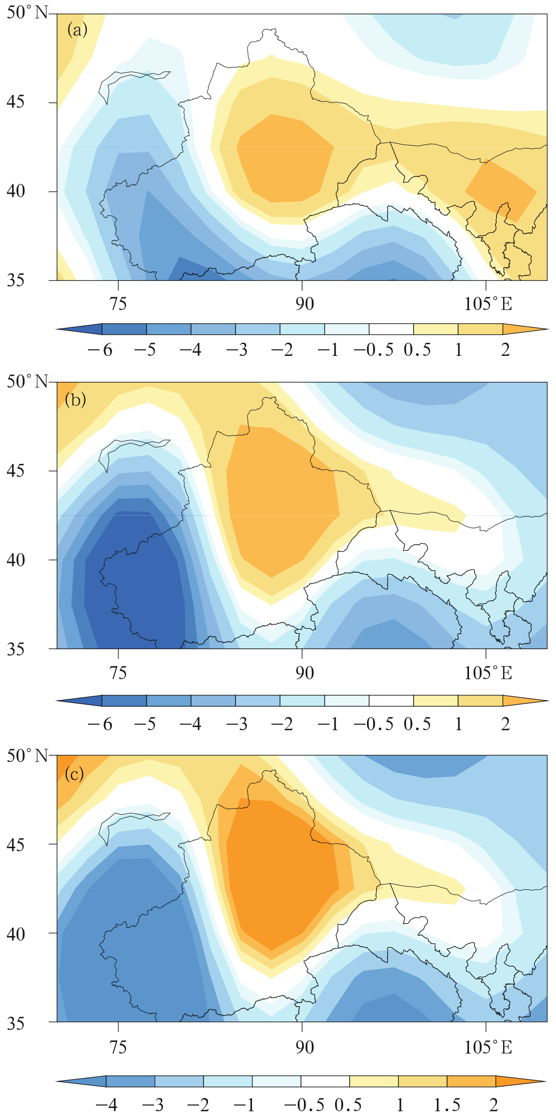

Fig. 4. JJA mean vertical velocity (10^{-2} Pa s^{-1}) at 500 hPa. (a) Reanalysis II, (b) NCEP GCM/SSiB, and (c) difference between NCEP GCM/SSiB and Reanalysis II.

the NMICC. The precipitation over NWC is sparse, but there are clear characteristics in terms of its distribution, i.e., little precipitation over the desert and Gobi areas. Two precipitation centers are located over northwestern Xinjiang, along the high elevation areas and the Hexi Corridor. These two precipitation areas receive the main summer precipitation over NWC (Guo and Li, 2006). Guo and Li (2006) described the role played by the Tianshan terrain, local rivers, and lakes in the high precipitation of northwestern Xinjiang. The precipitation located along the Hexi Corridor is mainly controlled by the subtropical synoptic system. The NCEP GCM/SSiB simulates the main patterns and also shows good performance in terms of the precipitation rate (Fig. 6b), which is less than approximately 0.4 mm day^{-1} in the Gobi region, around 0.8–1.2 mm day^{-1} in northwestern Xinjiang, and roughly 0.8–4.0 mm day^{-1} over the Hexi Corridor.

By and large, using the satellite-derived vegetation characteristics, the NCEP GCM/SSiB produces reasonable regional climate features over NWC.

4. Impacts of land surface processes on summer circulation and surface energy over NWC

In this section, case S2 using a map with marked land degradation in NWC and case S1 using the SSiB classification map (Fig. 1) are compared to examine the sensitivity of summer climate features in NWC to land surface processes.

In Fig. 1a, NWC is classified as grassland in northern Xinjiang, northwestern Inner Mongolia, the Hexi Corridor, and some surrounding central Asian countries and Mongolia. In case S2, most of those areas are defined as bare ground (Fig. 1b). The land cover changes in case S2 are generally consistent with those presented in Chen et al. (2009). The surface vegetation difference causes a substantial change in surface albedo. Figure 7 shows that, compared to case S1, case S2 leads to higher albedo around central-southern Xinjiang by more than 0.03, and by more than 0.05 in the Hexi Corridor and Mongolia. The net surface shortwave radiation in case S2 would decrease due to the higher surface albedo, and also the surface net heat flux decreases by 20–40 W m^{-2} in northwestern Xinjiang, the Hexi Corridor, and Mongolia (Fig. 8a). Because of no transpiration in case S2 over the degraded land area, the latent heat flux in the Hexi Corridor and in northern Xinjiang decreases by 10–20 and 10–60 W m^{-2}, respectively (Fig. 8c). However, due to the reduction of net radiation, the sensible heat flux in case S2 increases by approximately 20–30 W m^{-2} in northern Xinjiang and by 10–30 W m^{-2} in the Hexi Corridor to balance the energy budget. The

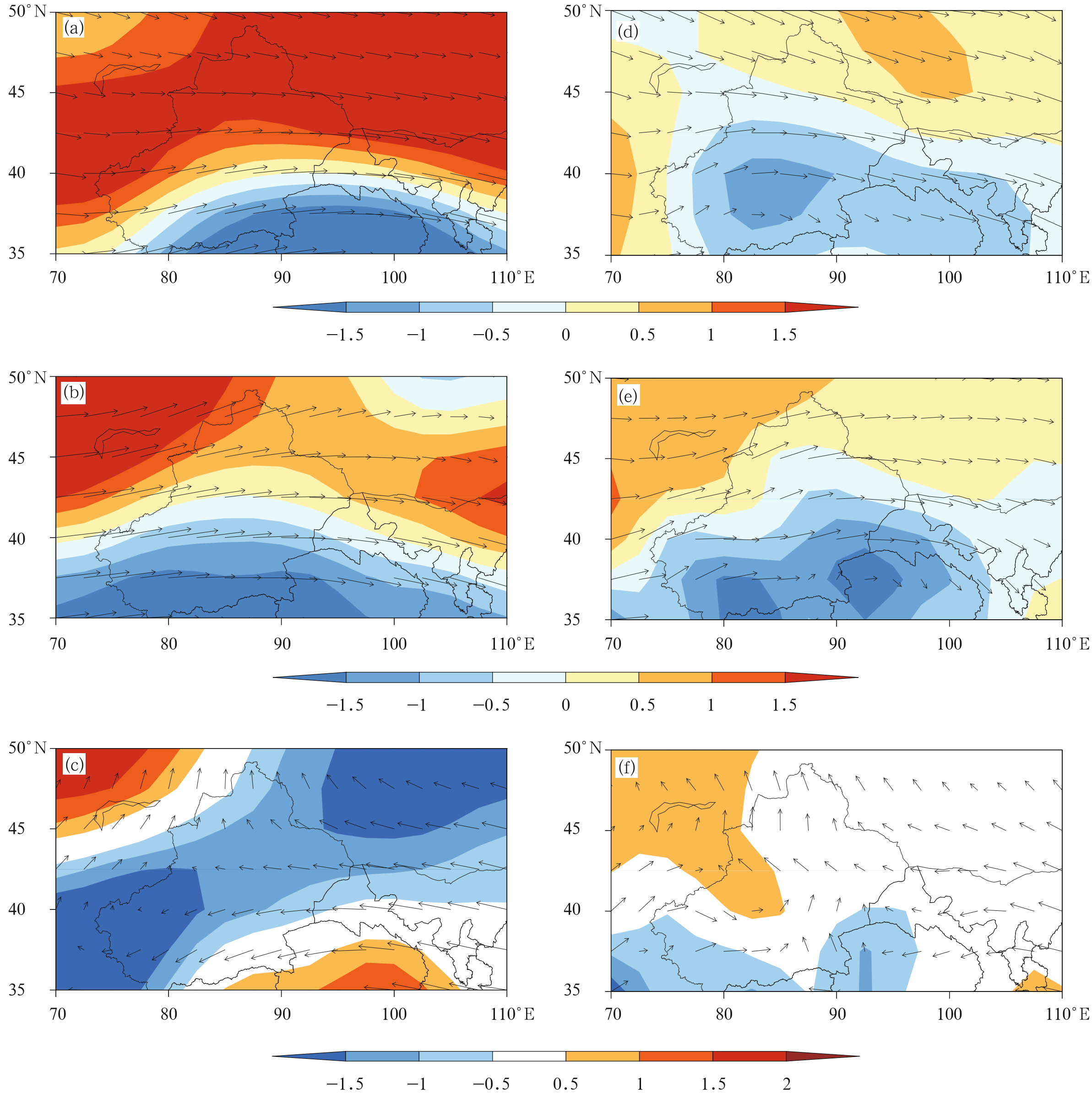

Fig. 5. JJA mean vorticity (10^{-6} s^{-1}) and wind (m s^{-1}) at (a, b, c) 200 and (d, e, f) 500 hPa. (a, d) Reanalysis II, (b, e) NCEP GCM/SSiB, and (c, f) difference between NCEP GCM/SSiB and Reanalysis II.

differences in surface energy balance change in these two areas are related to the soil moisture state. In case S2, soil moisture decreases greatly in northwestern Xinjiang, but very little in the Hexi Corridor (figure omitted), due to dry soil conditions in this semiarid area, which are consistent with a large reduction in latent heat flux in northwestern Xinjiang and less changes in the Hexi Corridor. Also, the surface temperature increases by 5–6℃ in northern Xinjiang and by 1–3℃ in the Hexi Corridor, due to the surface net radiation change in case S2 (Fig. 12a).

Changes in surface energy and water balance affect summer circulation over NWC. There are large changes in the vorticity field at 700 hPa (Fig. 9) in the Hexi Corridor and northwestern Xinjiang, which correspond to the area in NWC of large surface net radiation changes (Fig. 8a) in case S2.

Figure 9 shows that there are anomalous lower-layer anticyclonic and upper-level cyclonic circulations over northwestern Xinjiang, consistent with the large

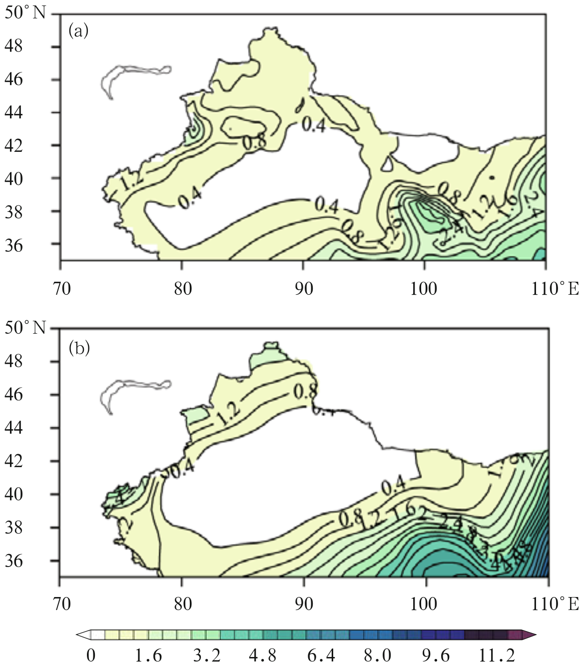

Fig. 6. JJA mean precipitation (mm day^{-1}). (a) observation and (b) NCEP GCM/SSiB.

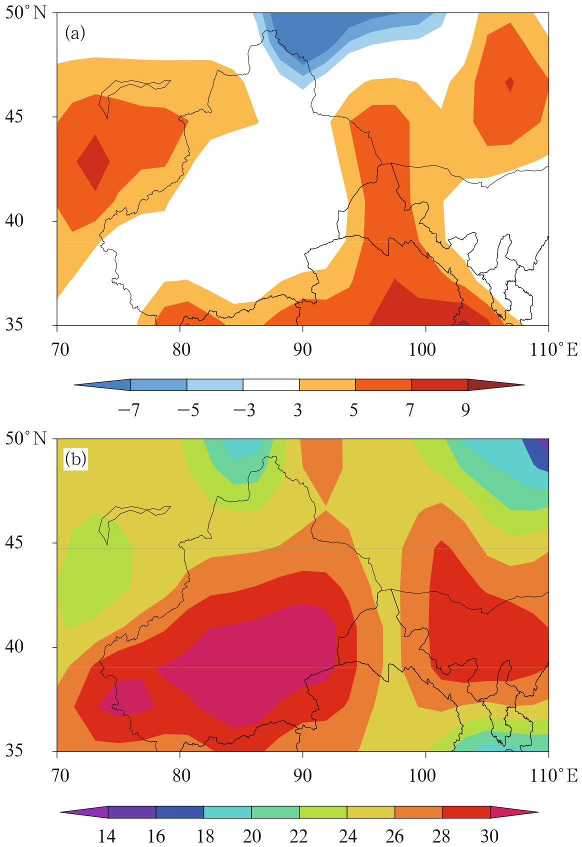

Fig. 7. JJA (a) difference of albedo between cases S2 and S1, and (b) surface albedo in case S1 in NWC.

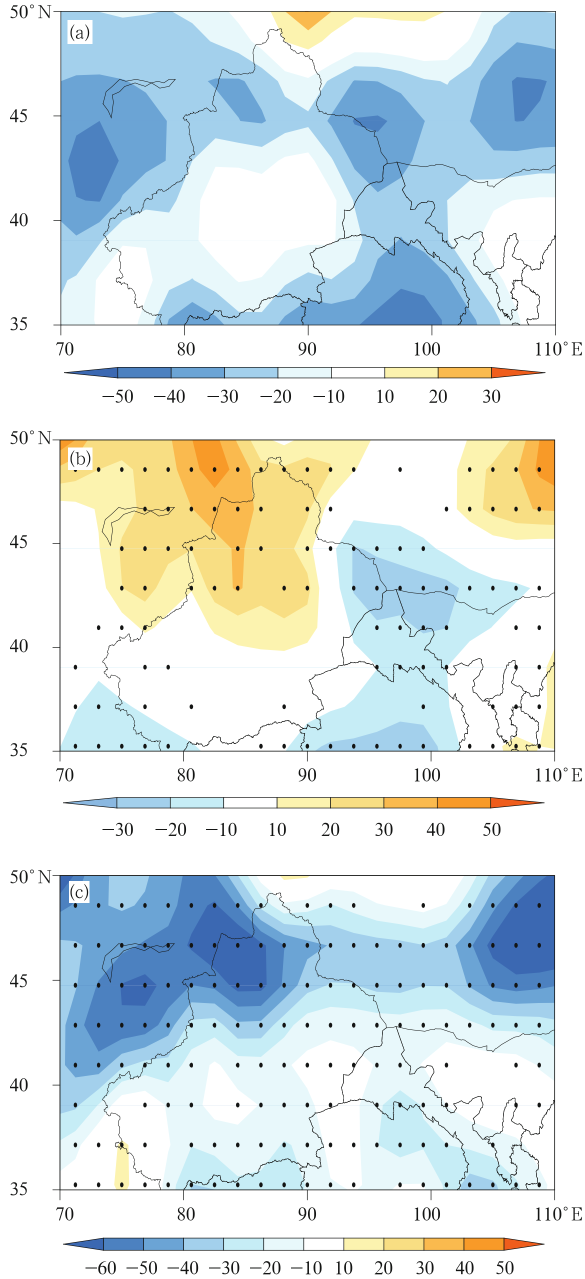

Fig. 8. JJA difference of (a) surface net radiation (W m^{-2}), (b) sensible heat flux (W m^{-2}), and (c) latent heat flux (W m^{-2}) between cases S2 and S1 in NWC. The dotted areas in (a–c) indicate the 90% confidence level.

reduction in surface latent heating. This circulation change is quite dominant over NWC and leads to lower-layer anomalous cyclonic circulation and anticyclonic circulations in the upper troposphere over the Hexi Corridor in case S2, where the change in surface latent heat fluxes is weaker. In a previous land cover

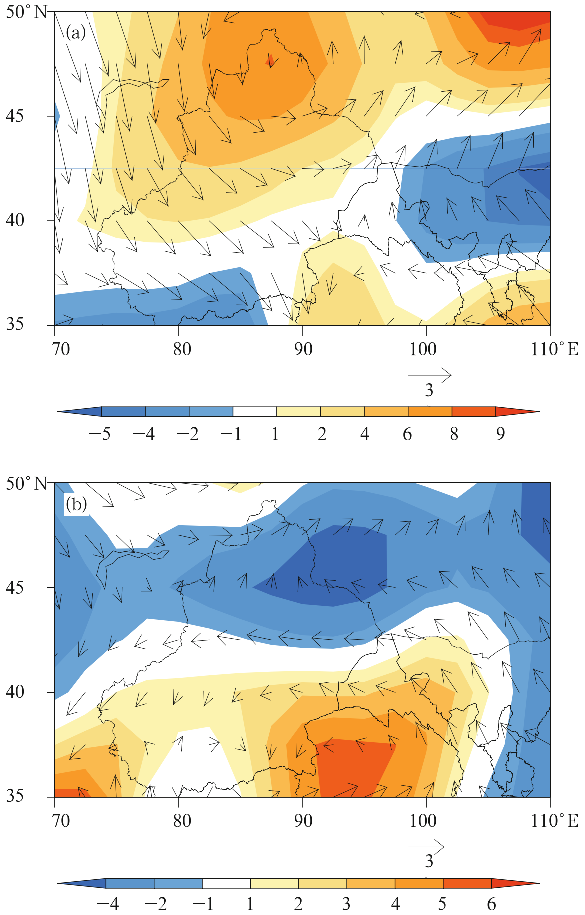

Fig. 9. JJA differences between cases S2 and S1 in NWC for wind (m s^{-1}) and vorticity (10^{-6} s^{-1}) at (a) 200 hPa and (b) 700 hPa.

change study (e.g., Xue, 1996), it was identified that the latent heat flux change makes a major contribution to the latent heating change in the lower and middle troposphere, and plays a major role in regional circulation change.

In addition, the moisture flux is convergent over the mountain areas of northwestern Xinjiang and weakly divergent over the Hexi Corridor in case S1 (Fig. 10a). In case S2, the moisture flux divergence in the Hexi Corridor changes to convergence (Fig. 10b) and the vertical descending motion becomes weaker (Fig. 11). Meanwhile, the moisture flux convergence in northern Xinjiang is much weaker and the descending motion is stronger. Therefore, in case S2, such summer circulation changes cause a decrease in precipitation over northern Xinjiang and an increase in rainfall over the Hexi Corridor in summer (Fig. 12b).

It can also be seen that there is an anomalous negative precipitation center over Mongolia (around 48°N, 105°E), where the change in the summer energy balance and circulations is consistent with that in northwestern Xinjiang. We do not discuss these changes in any further detail because they are beyond the scope of the present paper.

5. Conclusions and discussion

The major summer climate features of NWC and the performance of the NCEP/GCM SSiB in simulating these features over the region are presented in this study, in which satellite derived vegetation products are used. The possible effects of land surface processes over NWC on the summer energy balance and circulation are also evaluated with specified land cover

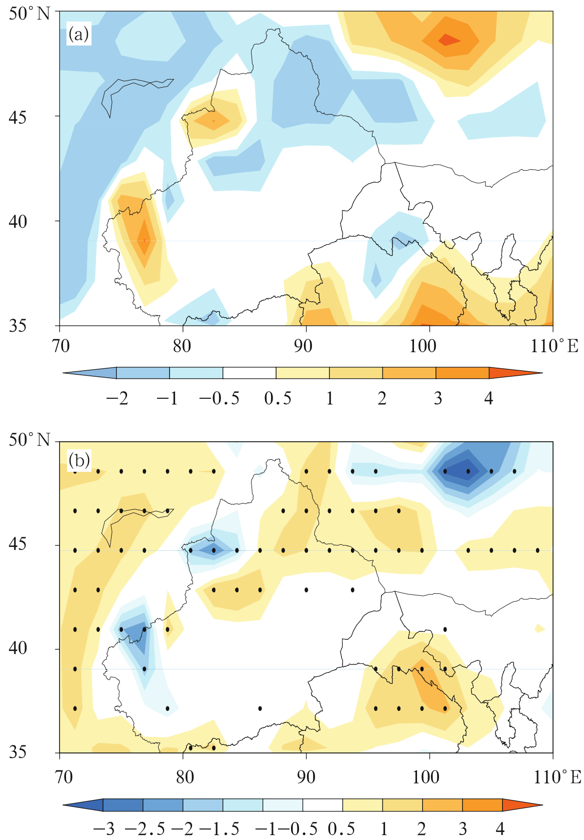

Fig. 10. JJA mean moisture flux (mm day^{-1}) (a) in case S1 and (b) the difference of moisture flux (mm day^{-1}) between cases S2 and S1 in NWC. The dotted areas in (b) indicate the 90% confidence level.

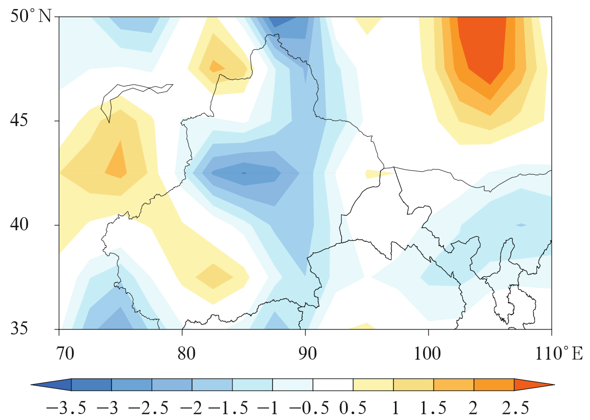

Fig. 11. JJA difference of vertical motion (Pa s^{-1}) at 500 hPa between cases S2 and S1 in NWC.

changes.

Based on the comparison with Reanalysis II, GSWP-2, and NMICC observational data, the NCEP GCM/SSiB reproduces the main energy balance and summer circulation features over NWC. The major climate features (high surface temperature and descending motion centers located in both the lower and middle troposphere; the cyclone in the upper troposphere and the anticyclone in the lower atmosphere) are all reproduced. The precipitation of NWC is mostly located in its high elevation areas. Both the model results and the GSWP-2 data illustrate that NWC acts as a "thermal pad" in summer. Further research will be conducted to explore the relationship of the deficiencies between the model simulation and observations/Reanalysis II data, and the surface thermal forcing due to inadequate land conditions and land surface parameterization by using recently available NWC field observation data and other satellite data.

The sensitivity of the summer energy balance and circulation over NWC to land surface processes is assessed for a land degradation scenario by comparing case S1 with case S2. When grassland in NWC and surrounding regions is changed to desert, the surface albedo increases by 3%–5%, leading to weaker surface thermal effects. In northern Xinjiang and surrounding regions, less latent heating causes stronger lower-level anomalous anticyclonic circulation and moisture flux divergence, and upper-level anomalous cyclonic circulation, leading to less summer precipitation there. On the other hand, the dry conditions in the Hexi Corridor and nearby areas produce less variation in latent heat flux. The circulation change to the north of this area is dominant and leads to lower-level cyclonic conditions, more convergence, weaker vertical descending motion, and thus a slight increase in precipitation over this region.

Our study is a preliminary investigation into the ability of the NCEP GCM/SSiB in simulating the basic summer energy balance and circulation features of NWC. We also assessed the effects of land surface processes in NWC and surrounding regions on the regional summer climate. There are a few studies that have focused on the impact of land cover change in NWC on the regional climate. Some, however, e.g., the study by Chen et al. (2009) based on the land cover change

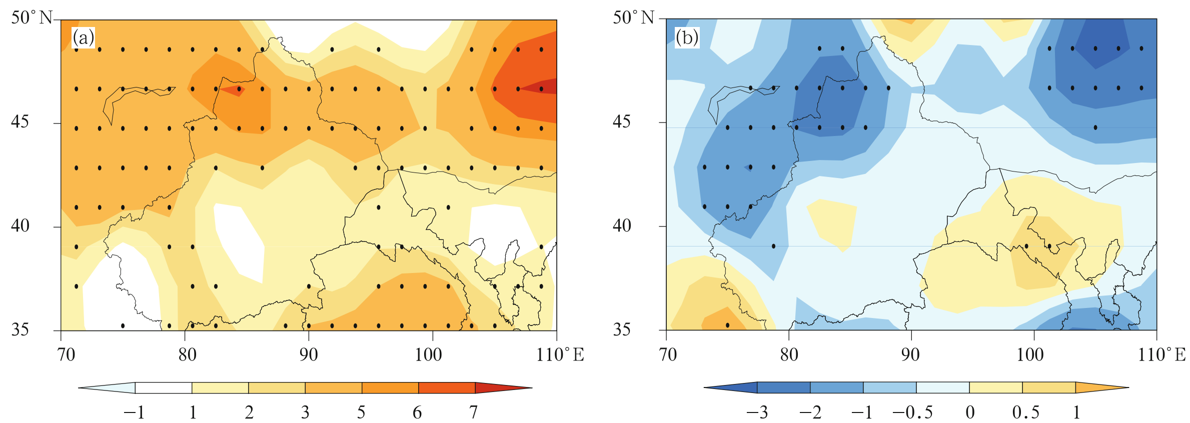

Fig. 12. JJA difference of (a) surface temperature (°C) and (b) precipitation (mm day^{-1}) between cases S2 and S1 in NWC. The dotted areas indicate the 90% confidence level.

between the 1990s and 1980s, have shown degraded areas in northern Xinjiang to become cooler with a slight increase in precipitation after land degradation, which is different from the findings of the present study. More studies with different models and experimental designs as well as better land cover change information, are necessary to further explore the impacts of land cover change on the climate of NWC.

When more observed data are available, we will apply them in further NWC climate simulations, along with satellite data. In order to improve our understanding of climate change in NWC and East Asia, we should also look to conduct further studies on the response of climate features, the water balance, and energy balance to land degradation based on more realistic land cover change data. This study shows that land cover change is one factor that may have a large impact on the regional climate of NWC. A comprehensive understanding of this and other factors, such as the greenhouse effect and the effects of aerosols, should contribute to a better understanding of past precipitation change in the region (e.g., Jin et al., 2005; Chen and Dai, 2009), as well as the production of more credible future projections.

Acknowledgments. The authors wish to thank Dr. Zhou Degang and Dr. Liu Yong from the Institute of Atmospheric Physics, Chinese Academy of Sciences, for providing the NMICC observation surface temperature data and precipitation data.

REFERENCES

Bueh Cholaw, Ji Liren, and Cui Maochang, 2002: Energy balance of land surface process in the arid and semi-arid regions of China and its relation to the regional atmospheric circulation in summer. *Climatic Environ. Res.*, **7**, 61–73. (in Chinese)

Buermann, W., J. Dong, X. Zeng, et al., 2001: Evaluation of the utility of satellite-based vegetation leaf area index data for climate simulations. *J. Climate*, **14**, 3536–3550.

Chen Dongdong and Dai Yongjiu, 2009: Characteristics of Northwest China rainfall intensity in recent 50 years. *Chinese J. Atmos. Sci.*, **33**, 923–935. (in Chinese)

Chen Junming, Zhao Ping, Liu Hongli, et al., 2009: Modeling impacts of vegetation in western China on the summer climate of northwestern China. *Adv. Atmos. Sci.*, **26**, 803–812.

Chen Lingzhi, 1994: The main type of vegetation and the protection strategy in China. *Advances in Biodiversity Research–Proceedings of the First National Symposium on the Conservation and Sustainable Use of Biodiversity.* China Science and Technology Press, Beijing, 1–7. (in Chinese)

Ding Yihui, Li Qiaoping, and Dong Wenjie, 2005: A numerical simulation study of the impact of vegetation changes on regional climate in China. *Acta Meteor. Sinica*, **63**, 613–621. (in Chinese)

Dirmeyer, P. A., X. Gao, M. Zhao, et al., 2006: GSWP-2: Multimodel analysis and implications for our perception of the land surface. *Bull. Amer. Meteor. Soc.*, **87**, 1381–1397.

Dong Anxiang, Bai Huzhi, and Lei Xiaobin, 2006: New development of arid climate research in Northwest China from 2001 to 2005 and main scientific problems. *Arid Meteor.*, **24**, 57–62. (in Chinese)

Dorman, J. L., and P. J. Sellers, 1989: A global climatology of albedo, roughness length and stomatal resistance for atmospheric general circulation model (SiB). *J. Appl. Meteor.*, **28**, 833–855.

Friend, A. D., and N. Y. Kiang, 2005: Land surface model development for the GISS GCM: Effects of improved canopy physiology on simulated climate. *J. Climate*, **18**, 2883–2902.

Fu, C. B., 2003: Potential impacts of human-induced land cover change on East Asian monsoon. *Global and Planetary Change*, **37**, 219–229.

Guo, J. Y., and Y. H. Li, 2006: Climatic characteristics of summer precipitation in northwestern China. *Arid Zone Research*, **23**, 489–494.

Hansen, M. C., R. S. DeFries, J. R. G Townshend, et al., 2000: Global land cover classification at 1-km spatial resolution using a classification tree approach. *Int. J. Remote Sens.*, **21**, 1331–1364.

Hu Yinqiao, and Gao Youxi, 1994: Some new understandings of land surface processes in arid area from the HEIFE. *Acta Meteor. Sinica*, **52**, 285–296. (in Chinese)

Huang Ronghui, Cai Rongsuo, Chen Jilong, et al., 2006: Interdecadal variations of drought and flooding disasters in China and their association with the East Asian climate system. *Chinese J. Atmos. Sci.*, **30**, 730–743. (in Chinese)

Jin, L. Y., J. L. Fu, and F. H. Chen, 2005: Spatial differences of precipitation over Northwest China during the last 44 years and its response to global warming. *Scientia Geographica Sinica*, **25**, 567–572.

Kanamitsu, M., W. Ebisuzaki, J. Woollen, et al., 2002: NCEP–DOE AMIP-II Reanalysis (R-2). *Bull. Amer. Meteor. Soc.*, **83**, 1631–1643.

Kang, H., Y. Xue, and G. J. Collatz, 2007: Impact assessment of satellite-derived leaf area index datasets using a general circulation model. *J. Climate*, **20**, 993–1015.

Kuchler, A. W., 1983: *World map of natural vegetation. Goode's World Atlas*. 16th ed., Rand McNally, New York, 16–17.

Long, X., C. H. Wang, J. Y. Guo, et al., 2003: Developments of study on climate and weather numerical simulation in arid area. *Arid Meteor.*, **21**, 59–65.

Los, S. O., and Coauthors, 2000: A global 9-yr biophysical land surface dataset from NOAA AVHRR data. *J. Hydrometeor.*, **1**, 183–199.

Matthews, E., 1984: Prescription of land-surface boundary conditions in GISS GCM II: A simple method based on high-resolution vegetation databases. NASA Tech. Memo., NASA TM-86096, 20.

——, 1985: Atlas of archived vegetation, land-use and seasonal albedo data sets. NASA Tech. Memo. NASA TM-86199, 53.

Shukla, J., C. Nobre, and P. Sellers, 1990: Amazon deforestation and climate change. *Science*, **247**, 1322–1325.

Wang Chenghai, Dong Wenjie, Wei Zhigang, et al., 2002: The simulation and analysis of land-surface processes on the typical arid area. *Plateau Meteor.*, **21**, 466–472. (in Chinese)

Wu Tongwen, and Qian Zhengan, 1996: The comparative analyses of differences between vertical circulation on north side of Tibetan Plateau in wet and dry summer and thermal effects of the plateau. *Acta Meteor. Sinica*, **54**, 558–568. (in Chinese)

Xu, Xingkui, Lin Zhaohui, Li Jianping, et al., 2002: Temporal-spatial characteristics of vegetation cover and desertification of China by using remote sensing data. *Prog. Nat. Sci.*, **12**, 46–50.

——, Chen Hong, and Zhang Feng, 2007: Temporal and spatial change of vegetation cover in the northwest of China and factors influencing vegetation variation. *Environ. Sci.*, **28**, 41–47. (in Chinese)

Xue, Y. K., 1996: The impact of desertification in the Mongolian and the Inner Mongolian grassland on the regional climate. *J. Climate*, **9**, 2173–2189.

——, P. J. Sellers, J. L. Kinter, et al., 1991: A simplified biosphere model for global climate studies. *J. Climate*, **4**, 345–364.

——, and J. Shukla, 1993: The influence of land surface properties on Sahel climate. Part I: Desertification. *J. Climate*, **6**, 2232–2245.

——, M. J. Fenessy, and P. J. Sellers, 1996: Impact of vegetation properties on U.S. summer weather prediction. *J. Geophys. Res.*, **101**, 7419–7430.

——, F. J. Zeng, K. Mitchell, et al., 2001: The impact of land surface processes on simulation of the U.S. hydrological cycle: A case study of 1993 US flood using the Eta/SSiB regional model. *Mon. Wea. Rev.*, **129**, 2833–2860.

——, H. -M. H. Juang, W. P. Li, et al., 2004: Role of land surface processes in monsoon development: East Asia and West Africa. *J. Geophys. Res.*, **109**, D03105, doi: 10.1029/2003JD003556.

Yatagai, A., and T. Yasunari, 1995: Interannual variations of summer precipitation in the arid/semi-arid regions in China and Mongolia: Their regionality and relation to the Asian summer monsoon. *J. Meteor. Soc. Japan*, **73**, 909–923.

Zhang Qiang and Zhao Ming, 1998: A numerical simulation of characteristics of land-surface process under interaction of oasis and desert in arid region. *Plateau Meteor.*, **17**, 335–346.

Zheng Yiqun, Qian Yongfu, Miao Manqian, et al., 2002a: The effects of vegetation change on regional climate. I: Simulation results. *Acta Meteor. Sinica*, **60**, 1–16. (in Chinese)

——, ——, ——, et al., 2002b: The effects of vegetation change on regional climate. II: Mechanisms. *Acta Meteor. Sinica*, **60**, 17–29. (in Chinese)

Zhou Liantong, 2009: A comparison of NCEP/NCAR, ERA-40 reanalysis and observational data of sensible heat in Northwest China. *Climatic Environ. Res.*, **14**, 9–20. (in Chinese)

—— and Huang Ronghui, 2006: Characteristics of interdecadal variability of the difference between surface temperature and surface air temperature in spring in arid and semi-arid region of Northwest China and its impact on summer precipitation in North China. *Climatic Environ. Res.*, **11**, 1–13. (in Chinese)

—— and ——, 2008: Interdecadal variability of sensible heat in arid and semi-arid regions of Northwest China and its relation to summer precipitation in China. *Chinese J. Atmos. Sci.*, **32**, 1276–1288. (in Chinese)